SIMULATIONS OF LIQUID FILM FLOWS WITH FREE SURFACE ON ROTATING SILICON WAFERS (ROWAFLOWSIM)

Markus Junk[(a)], Frank Holsteyns[(a)], Felix Staudegger[(a)], Christiane Lechner[(b)], Hendrik Kuhlmann[(b)], Doris Prieling[(c)], Helfried Steiner[(c)], Bernhard Gschaider[(d)], Petr Vita[(e)]

[(a)]Lam Research AG, Villach, Austria
[(b)]Institute of Fluid Mechanics and Heat Transfer, Vienna University of Technology, Austria
[(c)] Institute of Fluid Mechanics and Heat Transfer, Graz University of Technology, Austria
[(d)]ICE Strömungsforschung GmbH, Leoben, Austria
[(e)] Department Mineral Resources and Petroleum Engineering, University of Leoben, Austria

[(a)]markus.junk@lamresearch.com, [(b)]christiane.lechner@tuwien.ac.at, [(c)]prieling@fluidmech.tu-graz.ac.at, [(d)]bernhard.gschaider@ice-sf.at, [(e)]petr.vita@unileoben.ac.at

ABSTRACT

For application in the semi-conductor industries, the flow on a rotating disk (wafer) is studied numerically. A systematic validation of available variations of the Volume-of-Fluid (VoF) scheme for this two-phase flow problem is done. To make larger parameter variations of this problem with a moving fluid supply possible, a code based on the thin-film approximation is developed. To better understand possible physical mechanisms for the removal of nano-particulate contaminations from a wafer, another code to study the detachment of submicron particles exposed to shear flows is developed and validated. An immersed boundary method with direct forcing is implemented. The particle-wall interaction is treated with a soft contact model.

Keywords: two-phase flow, thin-film approximation, particle removal, immersed boundary method

1. INTRODUCTION

Lam Research AG develops and manufactures single-wafer wet-processing solutions for the semiconductor industry. Their core technology is based on spin processing tools. In a spin process chamber, specific cleaning, etching and stripping chemicals are applied onto the semiconductor substrates (wafers). During the process, the wafer is placed on a chuck with the side to be processed facing up. A nitrogen cushion protects the bottom side from any contact from any contamination. While the chuck and with it the wafer rotate, chemical mixtures can be applied to the wafer by means of a dispenser to form a liquid layer on the surface of the wafer. Dependent on the process step, the dispenser is either in a fixed position (centre or off-centre) or is moving across the wafer. The continuously supplied chemicals are spun off the wafer and collected in drain levels, which surround the chuck. Multiple drain levels are arranged on top of each other making several processing steps with different chemicals in one chamber possible. For this, the vertical position of the chuck can be changed. During the entire process, an air flow through the process chamber from the top prevents the chemical vapours from escaping the chamber into the surrounding environment. The air is exhausted through a duct in the side wall of the process chamber.

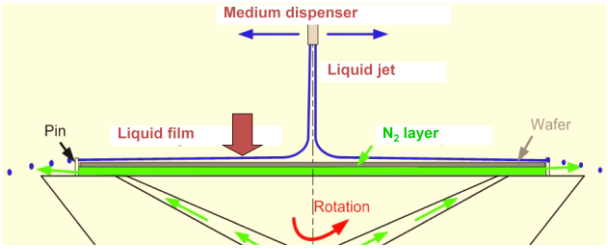

Figure 1: Sketch of a chuck, showing the moveable dispenser and the liquid jet, the N_2 cushion protecting the lower side of the wafer, and the ejection of droplets at its edge.

Semi-conductor industry has to face a number of challenges and continuously improve existing and develop new methods for processing due to decreasing dimensions (32nm and beyond) of the semi-conductor devices. One of these is the removal of nano-particulate contamination from wafer substrates without damaging high aspect ratio structures. Understanding the removal mechanisms in more detail is consequently an essential step in developing a reliable and efficient physical cleaning technique suitable for the 32 nm technology that can replace today's chemical cleaning technique. To meet these challenges, numerical simulations and especially computational fluid dynamics (CFD) simulations are getting more and more important. Lam Research is increasing its efforts to improve the simulation capabilities by close cooperation with universities. The cooperative project RoWaFlowSim (funded by the Austrian Research Promotion Agency FFG in the framework of the ModSim program) is part of these efforts and addresses flow related issues which are of high importance in the development process.

One subproject is related to thin film flow evolution and disintegration. A better understanding of liquid film flow, formation of droplets and ejection from the wafer is essential for the development of the

products, because they have a big impact on the quality and on the economic efficiency of the wafer processing. The formation of droplets and their movement in the airflow can lead to contamination on the wafer and to cross-contamination of the process media when the droplets enter the wrong drain level or are entrained in the airflow that is exhausted from the process chamber.

A second subproject is related to the transport of near-wall particles within the viscous sublayer of a laminar or turbulent boundary layer. The objective is to improve the understanding of particle adhesion and detachment by means of modelling and simulation. This will give an estimate of the minimum forces required to remove particles from a substrate, and lead to a better understanding of the larger scale flows, which are required for selective removal of contaminants, without damage to nanostructures. Understanding the basic effects will help to select physical mechanisms and to generate flows leading to jetting, micro-streaming, shock waves etc. (Fig. 2).

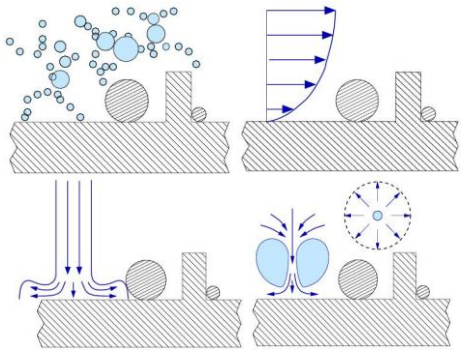

Figure 2: Physical mechanisms to generate controlled perturbations for particle removal: acoustic cavitation, acoustic streaming, droplet impact, laser bubbles.

2. FLOW ON A ROTATING WAFER

2.1. Numerical scheme

The work in this part of the project started with a systematic study of the suitability of several variations of the Volume-of-Fluid method (VoF), which is the method of choice for this kind of flows. The implementations available in the commercial code ANSYS Fluent and in the open-source code OpenFOAM were considered for this study. For a first comparison the numerical results of axisymmetric calculations with experimental results from the literature, a test case with simplified inflow conditions was chosen (Thomas, Fagri, and Hankey 1991).

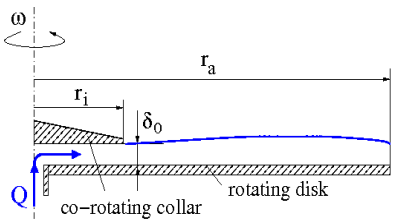

Figure 3: Inflow conditions for the first test case. The vertical jet is replaced by a horizontal inflow.

After comparing simulation results with the different available VoF schemes (Gschaider, Vita, Prieling, and Steiner (2010)), the HRIC scheme (in Fluent) and the Inter-γ scheme (in OpenFOAM) were selected as the most appropriate interface tracking schemes for further use in the project. Other schemes showed either too high smoothing of the interface or a physically questionable strong waviness of the instantaneous solutions and caused problems in the outer area of the disk where the film height becomes very thin. Therefore, these schemes are not used in the further work.

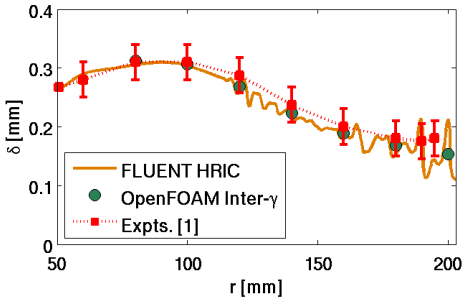

Figure 4: Comparison of the computed values for the instantaneous film thickness with experimental data for the case with horizontal inflow (water, flow rate 700l/min, rotation rate 200rpm).

2.2. Validation

For the more realistic case with a vertical inflow from a dispenser, the time-averaged numerical results always showed very good agreement with analytical solutions assuming a thin film approximation (Sisoev, Matar, and Lawrence 2003; Kim, and Kim 2009) for the axisymmetric case and in most cases also with the experimental data, if available. The simulations could also confirm that the profiles of the velocity components (based on 4th order polynomials) in the analytical solutions match very well those obtained in the 3D simulations sufficiently far away from the impingement region (Fig. 5). Discrepancies in some cases between the predicted time-averaged film heights and the corresponding experimental data may be partly attributed to uncertainties in the measured data.

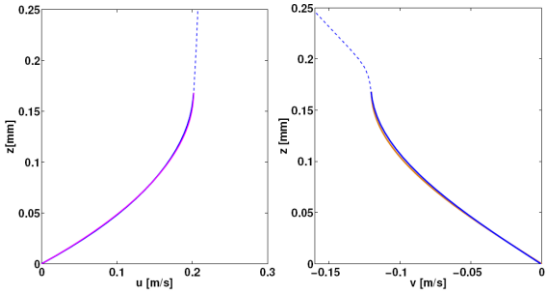

Figure 5: Profiles of the radial and azimuthal velocity at a radial position r=40mm (water, flow rate 0.36l/min, rotation rate 200rm).

Even in the case with axisymmetric boundary conditions, i.e. with central impingement, strong

disturbances in the circumferential direction especially in the outer part of the wafer are observed. This asymmetry in the flow, and the fact that in the real process tools, the liquid is often applied to the wafer from an off-centre positioned or even moving dispenser, make three-dimensional simulations necessary. The high computational costs require a carefully adapted design of the numerical mesh to resolve the motion of the very thin liquid structures. Simulations (with mesh sizes between 1 and 5 million cells) showed fairly good agreement (by visual comparison with high-speed images obtained in the laboratory) for the case with the lower rotational speed, where the 3D wavy structures in the outer region of the disk are relatively large (Fig. 6). For higher rotation rates these structures tend to break up into irregular small-scale wavelets, whose spatial resolution would require unaffordable mesh sizes. Nevertheless, the simulations capture the average mean values very well in all considered cases (Fig 7).

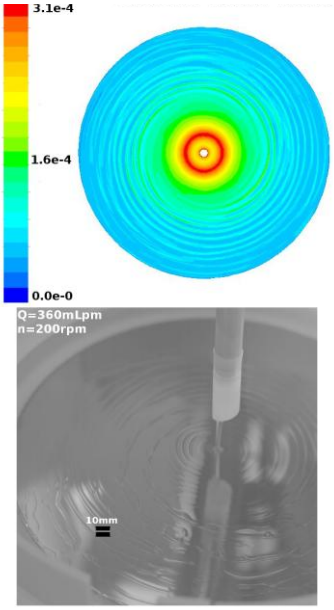

Figure 6: Surface waves in an axisymmetric setup with centred position of the dispenser in simulation (contours of film thickness) and experiment (water, flow rate 0.36l/min, rotation rate 200rpm)

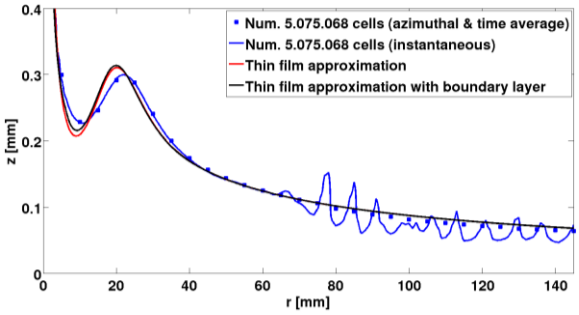

Figure 7: Comparison of computed instantaneous and averaged values of the film thickness (3D, Fluent) with results of an analytical solution based on a thin film approximation (water, flow rate 0.36l/min, rotation rate 200rpm).

The resulting computing times are still prohibitively high for systematic studies in the industrial use, even if a coarse base mesh is used and a dynamic grid adaption is applied where necessary. Thus, the applicability of 3D simulation is constrained to a small number of test cases and to a very limited range of operation conditions with relatively low rotational speeds. The costly 3D simulations are still highly valuable for the evaluation of some basic assumptions made in approximate solution approaches reducing the spatial dimensionality, as will be shown in the next section. Moreover, particular complex phenomena like a discontinuous wetted surface can only be captured by 3D simulations. This is seen from Fig. 8, where the 3D results reflect the formation of dry spots at the centre very well.

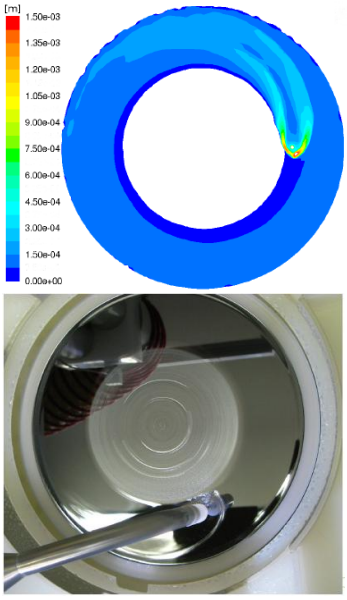

Figure 8: Occurrence of dry spots in a setup with static off-centre position of the dispenser (water, flow rate 0.3 l/min, rotation rate 60 rpm) in simulation (contours of film thickness) and experiment (note the reversed orientation of the rotation).

2.3. Thin film approximation

To make larger parameter studies of the flow on the wafer more feasible, it was decided to develop a numerical tool on a computationally less costly alternative, termed “2.5D” approach. This concept basically represents an integral method, reducing the simulation of the liquid flow to a 2D problem by solving the equations of motion in the thin film approximation (shallow water equations), neglecting the vertical momentum equation. This is justified by the small thickness of the liquid film compared to the dimensions of the wafer, and it seems to be a good candidate for most of the relevant operating conditions. The above mentioned analytical solutions are based on the same approximation; however, an analytical solution is impossible for off-centre or moving dispenser.

The dependent variables in this approach are the film height h and the vertically averaged film velocity $\bar{\boldsymbol{u}}$. For the vertical velocity profile, a 4th order polynomial ansatz is chosen. The coefficients of the polynomial

$$\boldsymbol{f}(\xi) = \boldsymbol{a_0} + \boldsymbol{a_1}\xi + \boldsymbol{a_2}\xi^2 + \boldsymbol{a_3}\xi^3 \quad (1)$$

with $\xi = x_3/h$ being the normalized vertical coordinate and the coefficients $\boldsymbol{a_i}(x_1, x_2)$ vectorial functions of the coordinates in the plane, are determined by the following set of boundary conditions at the wafer ($\xi = 0$) and at the free surface ($\xi = 1$):

$$f(\xi)|_{\xi=0} = \boldsymbol{u}_{\text{Wafer}},\ \left.\frac{\partial^2 f(\xi)}{\partial \xi^2}\right|_{\xi=1} = 0,\ \left.\frac{\partial f(\xi)}{\partial \xi}\right|_{\xi=1} = 0$$

$$\int_0^1 f(\xi)d\xi = \bar{\boldsymbol{u}} \quad (2)$$

Applying the thin film approximation, the resulting form of the momentum equation based on this velocity profile is given by

$$\frac{\partial}{\partial t}(h\bar{\boldsymbol{u}}) + \nabla(\bar{\boldsymbol{u}}\bar{\boldsymbol{u}}) = -\frac{1}{\rho}h\nabla(\rho|\boldsymbol{g}|h - \sigma\nabla^2 h) - \nu\frac{1}{h}\left.\frac{\partial f(\xi)}{\partial \xi}\right|_{\xi=0} \quad (3)$$

(σ: surface tension, ρ: density, ν: kinematic viscosity of the liquid, $\boldsymbol{g}$: gravity vector), which must be solved together with the continuity equation

$$\frac{\partial}{\partial t}h + \nabla(h\bar{\boldsymbol{u}}) = 0 \quad (4)$$

The programming of a flexible solver is based on an implementation of the Finite Area Method (FAM), a specialisation of the Finite Volume Method for film flows, by Tukovic and Jasak (2008) in a branch of OpenFOAM (OpenFOAM 1.6-ext, 2010).

The thin film approximation cannot be used in the vicinity of the impinging jet, where the flow is redirected and vertical momentum is converted to radial and circumferential momentum. Therefore, a combined approach must be used: the flow conditions close to the impingement region, which are the result of a fully 3D simulation, are imposed as a boundary condition. Outside this region, the flow is calculated based on the thin film approach. The full simulations have shown that the conversion of vertical momentum occurs in a rather confined area (typically less than 5mm radius, compared to 150mm wafer radius).

First tests of this concept assuming axisymmetric flow showed very good agreement with the results of the full 3D simulation with the VoF method. In the outer region, where the flow becomes non-axisymmetric and irregular, as indicated by the waviness in the instantaneous numerical results, good agreement with the averaged numerical results is still observed. The described profile assumptions are also used for the more complex cases with off-centre impingement (Fig. 9). For a moving dispenser, a static mesh turned out to be more economical and to yield better results than re-meshing based on the momentary dispenser position. With this code, it becomes now possible to calculate this practically most important cases on a time frame which is reasonable for industrial use (e.g. 3D VoF simulation: computing time up to 3 weeks on 4 cores for 1s real time; thin-film method: about 2 hours for 10s real time on 1 core of the same computer).

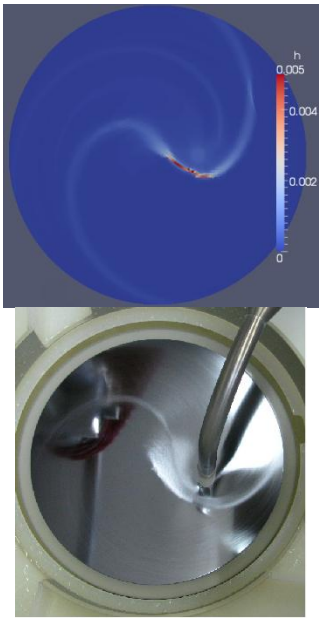

Figure 9: Simulation with the implemented thin-film approximation (contours of film thickness) for a test case with fixed off-centre position of the dispenser (offset 55mm, flow rate 2.8l/min, rotation rate 400 rpm).

2.4. Outlook

Present work in this part of the project concentrates on providing data for modelling the disintegration of the liquid film at the edge of the wafer and on the validation and the improvement of the implementation of the 2.5D concept. Extensions of this code, e.g. to calculate etch rates on the wafer, thus leading to a better modelling of the underlying industrial application, are under consideration.

3. PARTICLE MOTION

The objective of this sub-project is to numerically study the onset of particle motion under the influence of hydrodynamic forces and follow the particle after motion has set in. The idea is that physical mechanisms suitable to remove nano-particulate contamination from the substrate as e.g. acoustic cavitation generate local perturbations of the flow close to the surface of the wafer. Due to its small size, a submicron particle adhering to the substrate then essentially faces a simple

shear flow $\boldsymbol{u_0}(z,t)$ which exerts hydrodynamic forces $\boldsymbol{F_D}(t)$, $\boldsymbol{F_L}(t)$ and a torque $\boldsymbol{M_D}(t)$ on the particle as sketched in Fig. 10. By numerically exposing the particle to various profiles $\boldsymbol{u_0}(z,t)$ with different shear rates $\dot{\gamma}$, criteria for effective particle removal shall be established.

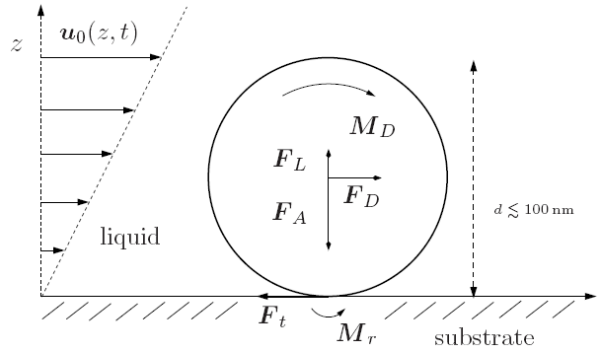

Figure 10: Model for particle removal: the nano-sized particle adhering to the substrate with adhesion force $\boldsymbol{F_A}$ faces a shear flow $\boldsymbol{u_0}(z,t)$, which exerts drag $\boldsymbol{F_D}(t)$, lift $\boldsymbol{F_L}(t)$ and a torque $\boldsymbol{M_D}(t)$ on the particle. $\boldsymbol{F_t}$ and $\boldsymbol{M_r}$ denote tangential friction and rolling resistance.

3.1. Numerical method

In order to numerically simulate the onset of motion and follow the particle after motion has set in, a direct numerical simulation is performed where the finite sized rigid particle fully couples to the fluid. To this end we implemented an immersed boundary method, following Uhlmann (2005) and Taira and Colonius (2007), into OpenFOAM. The incompressible Navier–Stokes equations are solved on a Cartesian grid covering a domain D which includes the region $P(t)$ occupied by the particle. The presence of the particle in the fluid is modelled with a volume force $\boldsymbol{f}(\boldsymbol{x},t)$ in the momentum equation,

$$\frac{\partial \boldsymbol{u}}{\partial t} + \boldsymbol{u}\cdot\nabla\boldsymbol{u} = -\nabla p + \nu\Delta\boldsymbol{u} + \boldsymbol{f}$$
$$\nabla\cdot\boldsymbol{u} = 0 \qquad (5)$$

where $p(x,t)$ denotes the pressure over density in the fluid and ν is the kinematic viscosity. $\boldsymbol{f}(\boldsymbol{x},t)$ has to be determined numerically such that the fluid velocity $\boldsymbol{u}(\boldsymbol{x},t)$ satisfies the no-slip condition $\boldsymbol{u}(\boldsymbol{x},t) = \boldsymbol{U}(t) + \boldsymbol{\Omega}(t)\times(\boldsymbol{x}-\boldsymbol{X}(t))$ at the surface of the particle $\partial P(t)$, where $\boldsymbol{U}(t)$ and $\boldsymbol{\Omega}(t)$ denote the particle's translational and angular velocities and $\boldsymbol{X}(t)$ is the centre of mass.

The momentum and the continuity equation are solved with icoFoam, OpenFOAM's standard solver for incompressible flow, which uses a PISO-like algorithm for pressure velocity coupling. During each pass in the corrector loop, before solving the Poisson equation for pressure, we require a corrected velocity to satisfy the no-slip condition on a set of Lagrangian marker points $\boldsymbol{X}_l$, which are regularly distributed on $\partial P(t)$. This condition yields a linear system of equations for a surface force $\boldsymbol{F}(\boldsymbol{X}_l)$. As the marker points $\boldsymbol{X}_l$ are not related to the Cartesian grid $\boldsymbol{x}_i$, interpolation and smearing operations are defined with the same regularized δ-function (see Peskin (2002) and Beyer and LeVeque (1992)).

Given a numerical solution to the above problem at a time t_n, the particle's equations of motion

$$\frac{d\boldsymbol{X}}{dt} = \boldsymbol{U}, \qquad M\frac{d\boldsymbol{U}}{dt} = \boldsymbol{F}_{\text{hydro}} + \boldsymbol{F}_{\text{body}} + \boldsymbol{F}_{\text{wall}}$$
$$I\frac{d\boldsymbol{\Omega}}{dt} = \boldsymbol{M}_{\text{hydro}} + \boldsymbol{M}_{\text{wall}} \qquad (6)$$

are solved, where M and I denote the mass and the moment of inertia of the (spherical) particle. $\boldsymbol{F}_{\text{body}}$ is a body force acting on the particle as e.g. gravity, which for a nano-sized particle is negligible compared to the adhesion force. $\boldsymbol{F}_{\text{hydro}}$ and $\boldsymbol{M}_{\text{hydro}}$ are computed directly from the surface force $\boldsymbol{F}(\boldsymbol{X}_l,t_n)$ and the fluid velocity $\boldsymbol{u}(\boldsymbol{x_i},t_n)$. $\boldsymbol{F}_{\text{wall}}$ and $\boldsymbol{M}_{\text{wall}}$ represent the force and torque the wall exerts on the particle and will be specified below.

The numerical implementation has been validated in 2D for standard test cases (Lechner and Kuhlmann (2010)). Validation in 3D is in progress. As an example, Fig. 11 shows the flow around a sphere in contact with the wall for a particle Reynolds number $\text{Re}_P = \dot{\gamma}d/(2\nu) = 2$, with $\dot{\gamma}$ the shear rate and d the diameter of the particle. The above algorithm easily can be extended to handle particles that deviate from spherical shape.

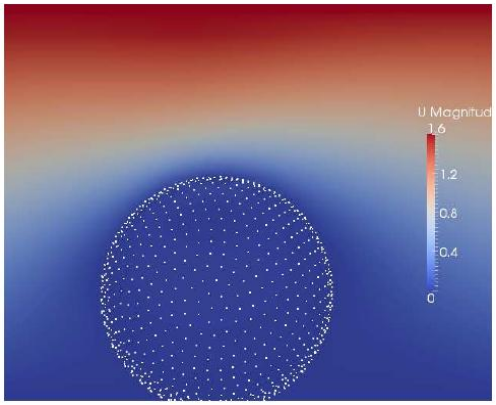

Figure 11: Direct numerical simulation of a (fixed) sphere in contact with a wall exposed to a linear shear flow. In this example the particle Reynolds number $\text{Re}_P = 2$. The no-slip boundary condition was enforced on the white points distributed on the surface of the sphere. The magnitude of the fluid velocity is shown on the plane y = const through the centre of the sphere with a scale $V = \dot{\gamma}d$.

3.2. Interaction with a wall

The hydrodynamic forces will cause motion of the particle in form of lift-off, sliding or rolling if they overcome the contact forces comprising adhesion, tangential friction, rolling and torsion resistance. The forces and torques describing the particle-wall interaction are given by

$$\boldsymbol{F}_{\text{wall}} = \boldsymbol{F}_n + \boldsymbol{F}_t + \frac{RM}{I + R^2 M}\boldsymbol{n} \times \boldsymbol{M}_r$$
$$\boldsymbol{M}_{\text{wall}} = R\boldsymbol{n} \times \boldsymbol{F}_t + \frac{I}{I + R^2 M}\boldsymbol{M}_r + \boldsymbol{M}_t \qquad (7)$$

where R denotes the radius of the particle and $\boldsymbol{n}$ is the unit normal to the wall pointing from the fluid region outside. The normal part $\boldsymbol{F}_n$ includes a repulsive force opposing elastic deformation and the attractive adhesion force. Depending on the elastic properties and the size of the particle a family of models ranging from the Johnson-Kendall-Roberts model to the Derjaguin-Muller-Toporov model (see e.g. Johnson and Greenwood (1997)) is appropriate to describe $\boldsymbol{F}_n$.

Tangential friction $\boldsymbol{F}_t$ resists the relative motion of the contact area and the wall until static friction is overcome and sliding sets in. For (sub)-micron particles sliding friction is described by $\boldsymbol{F_t} = -\tau_s A_c \hat{\boldsymbol{U}}_c$, with τ_s the shear stress of the contact, A_c the contact area and $\hat{\boldsymbol{U}}_c$ the unit vector in direction of the relative velocity. Similarly the critical rolling resistance could be modelled as $\boldsymbol{M}_r = -\tau_r R A_c \hat{\boldsymbol{\Omega}}$ with τ_r the rotational friction coefficient and $\hat{\boldsymbol{\Omega}}$ the unit vector in direction of the angular velocity (see e.g. Sitti (2004)). τ_r and τ_s have to be determined experimentally for the materials under consideration. The contact area A_c can be derived from the adhesion models if the work of adhesion is known. $\boldsymbol{M}_t$ denotes the torsion resistance. Combining Eqs. (5) and (6) and assuming equilibrium, the limit of sliding or rolling friction would be reached if the hydrodynamic forces satisfy the following inequalities

$$\left|\frac{2}{7}\boldsymbol{F}_D + \frac{5}{7R}\boldsymbol{n} \times \boldsymbol{M}_D\right| \geq \tau_s A_c \quad \Longrightarrow \text{sliding}$$
$$|-\boldsymbol{M}_D + R\boldsymbol{n} \times \boldsymbol{F}_D| \geq \tau_r A_c \quad \Longrightarrow \text{rolling} \qquad (8)$$

As a first step for a stationary linear shear flow at very small particle Reynolds numbers Re_P, the expressions derived by O'Neill (1968) can be used to approximate drag and torque, $|\boldsymbol{F}_D| \simeq 16.031\ \text{Re}_P \rho\, \nu^2$ and $|\boldsymbol{M}_D| \simeq 5.93\, R\ \text{Re}_P \rho\, \nu^2$, where ρ denotes the density of the liquid (note, that there is a typo in the paper concerning the torque, which misses a factor 1/2). This would yield the following conditions for the onset of sliding respectively rolling

$$0.345\ \text{Re}_P \rho\, \nu^2 \gtrsim \tau_s A_c,$$
$$21.96\ \text{Re}_P \rho\, \nu^2 \gtrsim \tau_r A_c \qquad (9)$$

3.3. Outlook

At present, the 3D implementation is being validated. The next step will be the comparison with experimental data (onset of motion of well defined particles in a shear flow) which are being generated within another cooperative project by Lam Research AG.

ACKNOWLEDGMENTS

The funding by the Austrian Research Promotion Agency (FFG) within the ModSim program (project number 819320) is gratefully acknowledged.

REFERENCES

Beyer, R.P., LeVeque, R.J., 1992. Analysis of a one-dimensional model for the immersed boundary method. *SIAM Journal on Numerical Analysis*, 29, 332-364.

Gschaider, B., Vita, P., Prieling, D., Steiner, H., 2010. Liquid coverage of a rotating disk. *5th OpenFOAM workshop*, Göteborg (Sweden). Slides

Johnson, K.L., Greenwood, J.A., 1997. An adhesion map for the contact of elastic spheres. *Journal of Colloid and Interface Science*, 192, 326-333.

Kim, T.S., Kim, M.U., 2009. The flow and hydrodynamic stability of a liquid film on a rotating disc. *Fluid Dynamics Research*, 41, 1-28.

Lechner, C., Kuhlmann, H.C., 2010. Development of a code for the direct numerical simulation of particles detaching from solid walls by hydrodynamical forces. In: M. Sommerfeld, ed. *Proceedings of the 12th workshop on Two-Phase Flow Predictions, Halle (Germany).*

O'Neill, M.E., 1968. A sphere in contact with a plane wall in a slow linear shear flow. *Chemical Engineering Science*, 23, 1293-1298.

Peskin, C.S., 2002. The immersed boundary method. *Acta numerica*, 11, 479-517.

Sisoev, G.M., Matar, O.K., Lawrence, C.J., 2003. Axisymmetric wave regimes in viscous liquid film flow over a spinning disk. *Journal of Fluid Mechanics*, 495, 385-411.

Sitti, M., 2004. Atomic force microscope probe based controlled pushing for nanotribological characterization. *IEEE/ASME Transactions on Mechatronics*, 9, 343-349.

OpenCFD, 2010. OpenFOAM 1.7.1 Available from: http://openfoam.com

The OpenFOAM-Extend Project, 2010. OpenFOAM 1.6-ext. Available from: http://www.extend-project.de

Taira, K., Colonius, C., 2007. The immersed boundary method: A projection approach. *Journal of Computational Physics*, 225, 2118-2137.

Thomas, S., Fagri, A., Hankey, W., 1991. Experimental analysis and flow visualization of a thin liquid film a stationary and rotating disk surface. *ASME Journal of Fluids Engineering*, 113, 73-80.

Tukovic, Z., Jasak, H., 2008. Simulation of free-rising bubble with soluble surfactant using moving mesh finite volume/area method. *6th International Conference on CFD in Oil & Gas, Metallurgical and Process Industries, SINTEF/NTNU*, 10-12 June, Trondheim (Norway).

Uhlmann, M., 2005. An immersed boundary method with direct forcing for the simulation of particulate flows. *Journal of Computational Physics*, 209, 448-476.